Journal of
Applied Remote Sensing

Three-date landsat thematic mapper composite in seasonal land-cover change identification in a mid-latitudinal region of diverse climate and land use

Priyakant Sinha
Lalit Kumar
Nick Reid

SPIE

Three-date landsat thematic mapper composite in seasonal land-cover change identification in a mid-latitudinal region of diverse climate and land use

Priyakant Sinha, Lalit Kumar, and Nick Reid
University of New England, Ecosystem Management, School of Environmental and Rural Science, Armidale 2351, NSW, Australia
psinha@une.edu.au

Abstract. Land-use and land-cover (LULC) classification accuracy in different seasons is not constant due to seasonal variations in spectral characteristics of different land-cover classes. This study addresses the problem of selecting a suitable season for mapping land-cover and identifying changes between seasons of midlatitude (29 deg 30′ to 31 deg 0′S) region of distinctive summer and winter rainfall, a broad altitudinal range, a temperate to subtropical climate and diverse land uses (e.g., summer and winter crops and nature conservation). Six landsat thematic mapper (TM) images from 2007 to 2009 were used taking three sequential three-date composites for seasonal change detection. January (midsummer) was the most suitable season in providing high spectral separability between most classes. The study demonstrates the means for improving LULC classification accuracy through the selection of optimal season for individual LULC class mapping and also provides a method of combining two or more classifications using referential refinement technique to generate aggregate LULC map of the region. © *2012 Society of Photo-Optical Instrumentation Engineers (SPIE).* [DOI: 10.1117/1.JRS.6.063595]

Keywords: aggregation; land-use; referential refinement; transformation.

Paper 12075 received Mar. 20, 2012; revised manuscript received Sep. 10, 2012; accepted for publication Sep. 25, 2012; published online Oct. 30, 2012.

1 Introduction

Land-use and land-cover (LULC), along with land management practices, have a profound impact on Australia's natural resources, the environment and agricultural production.[1] Land-use information provides input to planning and implementing land-use practices, and assessing the suitability of changes in land-use with respect to biodiversity, climate, soil and water availability.[2–6] Land-use change detection and reporting are critical for evaluating and monitoring trends in natural resource conditions.[7] However, investigation of the amount of change depends on the availability of consistent time series of land-use data capable of highlighting the change in targets of interest.[8] In order to understand land-use in any given year, it is important to identify the activities carried out in different seasons. This, in turn, provides insight into the extent of land dedicated to cropping and other primary production activities in different seasons[9] and is the basis for identifying the pattern and extent of LULC change from one season to another.

For better understating of seasonal dynamism and achieving high classification accuracy, multiseason remote sensing data are useful. For example, Schriever and Congalton[10] analyzed May (bud break), September (full leaf) and October (senescence) thematic mapper (TM) images to generate high-quality forest-cover maps with varying phenological information. They concluded that time of the year significantly affected cover-type classification accuracy in seasonal environments. In a similar study, Wolter et al.[11] used multispectral scanner (MSS) and TM data in different seasons to capture phenological changes in various tree species, achieving an overall accuracy of 83.2% and a forest classification accuracy of 80.1%. Most seasonal LULC change studies involve the use of images of nonsequential dates and also do not provide annual estimates of LULC in a given year. Furthermore, studies based on medium resolution satellite data using

0091-3286/2012/$25.00 © 2012 SPIE

sequential dates are limited either to accuracy assessment of classification results from one or more bands (e.g., Ref. 12) or mapping of a particular cover type e.g., forest (e.g., Refs. 11 and 13) or summer and winter grasses (e.g., Ref. 14) and not focused on entire LULC classes in a given region.

The most commonly used methods for extracting land-cover change from satellite images can be either through image-to-image comparison or map-to-map comparison.[15] General reviews of different algorithms under these two categories are given elsewhere.[16,17] While the image-to-image comparison does not provide details about the nature of LULC change, the map-to-map comparison, involving post classification comparison (PCC) of two separate dates classifications, explains a full matrix of land-cover changes, and is sometimes preferred over the former (e.g., Ref. 18). The scope of PCC in identifying class-wise changes between two periods can be extended to three or more dates by using geographical information system (GIS) technique (e.g., Refs. 19 and 20). Raster GIS is useful for integrating and analyzing multitemporal land-cover data and identifying changes using pixel-based logical operations. However, the technique and efficiency of classification of images of different dates determine the success and effectiveness of this method. RGB-NDVI[21] is another technique employed for land-cover change detection with three sequential dates of NDVI. The process is simple in design, changes are easy to interpret, and the technique can be automated through unsupervised classification for the quantification of changes.[22,23]

The current study addressed the issue of using sequential date images in determining seasonal variations in different LULC categories and providing annual estimates of land-cover in a given year. The key objectives of this study were: (a) to select the optimal season for mapping individual land-cover types; (b) to assess the effectiveness of sequential-date images in identifying seasonal variations in LULC; and (c) to apply referential refinement and aggregation techniques to results for three seasons to produce an annual estimate of land-cover in the region. The study emphasizes the importance of considering seasonal variations in the spectral characteristics of individual land-cover categories, and the fact that optimal selection of a particular month for mapping individual classes can have a large impact on the accuracy and reliability of the resulting classification.

2 Study Region

2.1 *Location*

The study region was in northern NSW, Australia, between 29 deg 30′S and 31 deg 0′S latitude and 150 deg 15′E and 152 deg 15′E longitude, covering 34200 km^2 and an altitude ranging from 260 to 1400 m asl (Fig. 1). The region included major parts of the New England Tablelands and

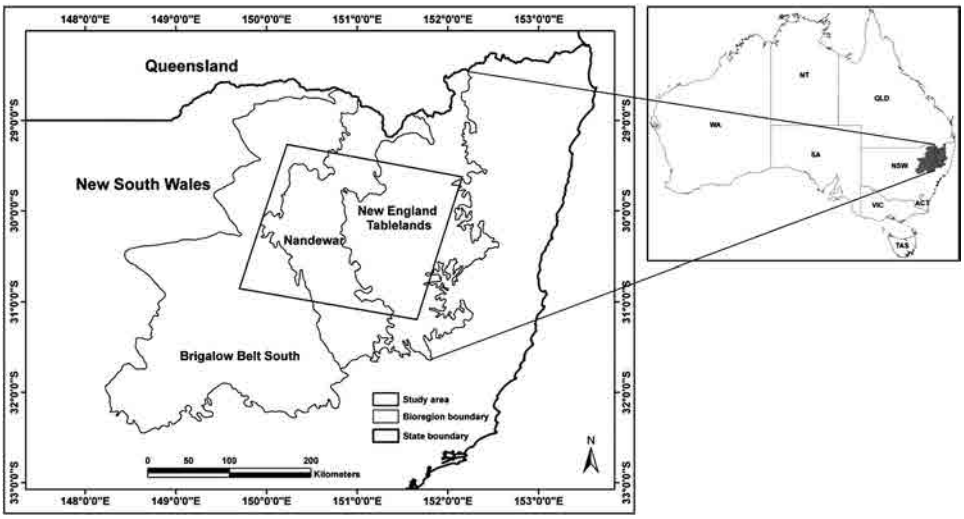

Fig. 1 Location of the study region.

Nandewar bioregions and a small portion of the Brigalow Belt South bioregion,[24] spanning the Northern Tablelands, the North-West Slopes, and the North-West Plains of NSW, respectively. The climate is subhumid and is temperate in the eastern tablelands portion of the region with a mean annual rainfall of 800 to 1000 mm, a January maximum of 23°C to 26°C and a July minimum of 0°C to 2°C.[25] On the plains in the west of the region, mean annual rainfall is about 550 to 650 mm, with a January maximum temperature of 33°C and a July minimum temperature of 5°C. The wide variety of duplex and gradational soils mainly support open forests and woodlands dominated by eucalypts where the vegetation has not been cleared or thinned for cropping and grazing. Rainfall decreases from east to west across the region. The dual summer-winter rainfall and temperature variations from warm summer to frosty winter support herbaceous vegetation dominated by both summer-active and winter-active plants (native and introduced).

2.2 *LULC Identified in the Region*

The Australian Land Use and Management Classification (ALUMC) scheme developed by Baxter and Russell[26] was used. ALUMC has a three-tiered hierarchical structure arranged in terms of the degree of modification and impact on the natural state.[1] Primary and secondary classes relate to land-use: the prime use of land, defined in terms of the management objectives of the land manager. Tertiary classes include commodity groups, commodities, land-management practices, and vegetation information. In the present study, secondary-level classification was adopted with the identifications of nine LULC classes viz. Evergreen forest (EF), evergreen woodland (EW), native pasture (NP), Improved pasture-high density (IP-HD), improved pasture-low medium density (IP-LMD), crop land (CL), fallow land-black soil (FLBS), fallow land grey/red soil (FLGRS) and waterbody (WB). Table 1 summarizes the descriptions of LULC identified in the region.

Table 1 LULC identified in the study region and their descriptions.[1]

LULC	Descriptions
Sclerophyll evergreen forest (EF)	Mostly strict nature reserves, national parks and other protected landscapes consisting of evergreen forest dominated mainly by *Eucalyptus* species
Sclerophyll evergreen woodland (EW)	Characterized by low to medium tree density, mostly on rugged steep rocky hills and peaks, dominated mainly by *Eucalyptus* species
Native pasture (NP)	Mainly native grassland on slopes with unproductive soils, supporting low livestock productivity throughout year
Improved pasture (high density) (IP-HD)	Well maintained grasslands or pastures used for livestock production, based on active modification or replacement of native vegetation
Improved pasture (low to medium density) (IP-LMD)	Similar to IP-HD except lower vegetation density
Crop land (CL)	Land under crop at time of image capture
Fallow or ploughed land (black soil) (FLBS)	Agricultural lands with black soil where crop production is carried out but fallow at time of image generation
Fallow or ploughed land (grey/red soil) (FLGRS)	Agricultural land with no standing crop and where soil was grey or red
Waterbody (WB)	All forms of waterbodies

3 Materials and Methods

3.1 *Remote Sensing Data Used*

Multitemporal, multispectral digital Landsat 5 TM data for six dates (January 2007, May 2007, August 2007, September 2007, March 2008, and November 2009; WRS2 path 90, row 81), were used for the purposes of land-cover classification and change detection analysis. No cloud-free data were available for March and November months in the year 2007; therefore images of the nearest available dates (March 2008 and November 2009) were used instead. TM data records energy in the visible bands (B1-blue: 0.45 to 0.52 μm; B2-green: 0.52 to 0.60 μm; and B3-red: 0.63 to 0.69 μm), near-infrared band (B4: 0.76 to 0.90 μm), mid-infrared bands (B5: 1.55 to 1.75 μm and B7: 2.08 to 2.35 μm) and thermal infrared band (B6: 10.4 to 12.5 μm) with a spatial resolution of 30 m for bands 1 through 5, 7, and 120 m for band 6, with a revisit coverage of 16 days. Except for thermal band (B6), all other TM bands, (B1 to B5, B7) were used in image processing. The images were geo-referenced to the WGS-84 UTM coordinate system. All work was undertaken using ENVI (4.5) ITT Visual information solution, USA (www.ittvis.com). Each Landsat scene comprised approximately 80% of the New England Tablelands and Nandewar Bioregions of NSW (Fig. 1). Images were selected in all four seasons, summer (January), autumn (March and May), winter (August), and spring (September and November) to compare land-cover classes and phenological differences between scenes. Intra-annual changes in land-cover classes at latitude 30 deg S (in a temperate to subtropical climate) are mostly due to different vegetation and management response to seasonal changes in temperature as well as to varying amounts of seasonal rainfall across all four seasons. The region is characterized by summer and winter rainfall, with only a slight dominance of summer rain. In spring, winter-active, and year-long growing crops and pasture plants and winter weeds are all in full growth mode until late spring, and become dormant during the hot dry months of summer.[27] Further, the summer crops (mainly cotton) and pastures (native and introduced) have a growing period from mid-spring to mid-summer and being harvested in autumn. The preparation of sowing of winter crops (mainly wheat) starts in autumn, which continues to grow until mid-spring before being harvested in late spring. Therefore, two major transition periods when major changes occurred in vegetation cover were observed between the seasons, the first transition from winter through spring up to early summer and the second transition was observed between early spring through summer and then up to autumn.[27] In mid-summer the reliability of the summer irrigation of crops and pastures, and the reliability of at least some summer rainfall stimulates growth in the range of sown and native pasture types present, as well as access to deep soil moisture by evergreen forests and woodlands. Thermal Band 6 was not used in any of the image processing due to its poor spatial resolution. Figure 2 shows flow chart explaining various image processing and statistical analysis steps carried out in this study.

3.2 *Image Normalization*

All six TM image Digital Numbers (DNs) were converted to top-of-atmosphere (TOA) reflectance values using the equation of Chander and Markham.[28] This provides a standardized measure directly comparable between images[29] and does not account for atmospheric interference. A relative radiometric normalization was performed to make the temporal images acquired at different dates radiometrically comparable by normalizing the variation in solar illumination conditions, atmospheric conditions and other properties.[7,30] The November 2009 image was selected as the base image because of its highest sun angle and minimum shadow effect. A linear regression method[31,32] was applied to January (2007), March (2008), May (2007), August (2007), and September (2007) imageries to match a given pixel's DN with the corresponding pixel's DN on the November (2009) base image. Normalization targets were selected from a wide range of pixel brightness values as suggested by Eckhardt et al.[31] to develop more accurate regression models. Eight normalization targets (e.g., deep-clear water: 2 sites; settlements: 2 sites; black bare soil: 3 sites; and bright clay/salt affected soil: 1 site) representing nonvegetated extremes of brightness values were selected through visual interpretation and GPS based field survey.

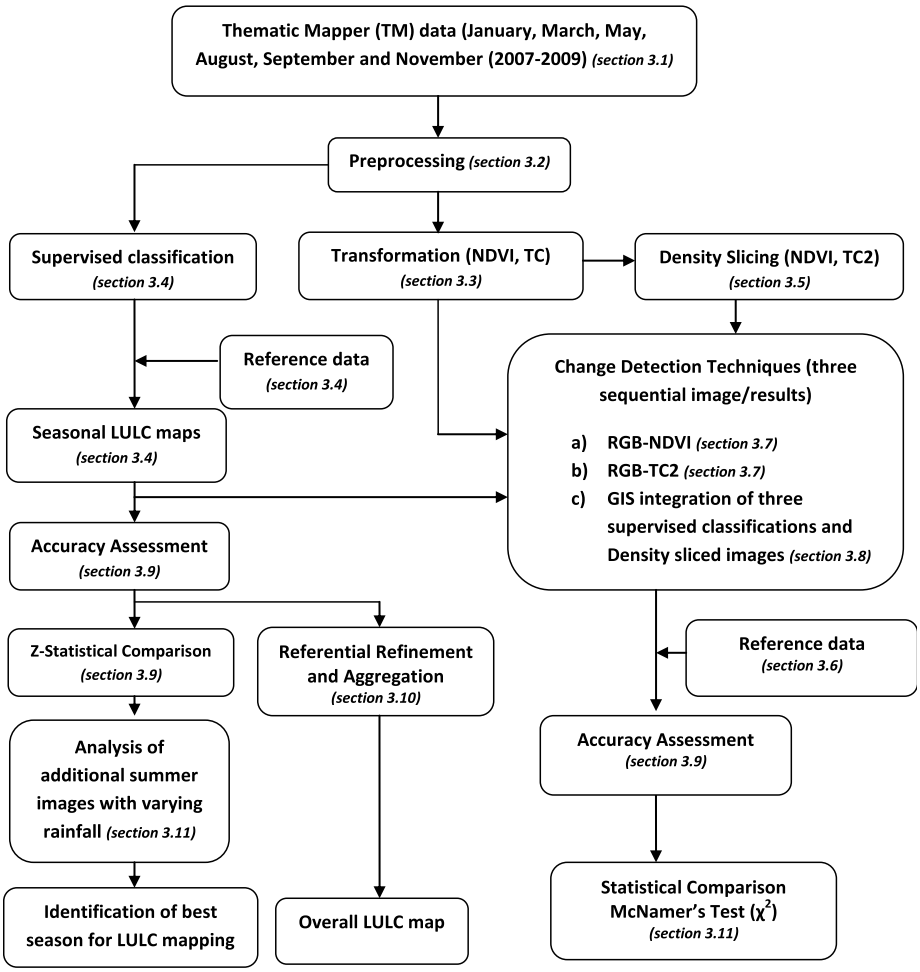

Fig. 2 Flow chart explaining various image processing and statistical analysis steps carried out in this study.

3.3 *Image Transformation*

3.3.1 *Normalized difference vegetation index*

NDVI was computed for assessing the type, extent, and condition of vegetation in the study region as a part of land-use investigations and to separate vegetated and nonvegetated areas. The NDVI was calculated as a ratio between measured reflectivity in the red and near-infrared portions of the electromagnetic spectrum. Vegetation with high leaf biomass, canopy closure, or leaf area is associated with higher NDVI values.[21,33] The ease with which NDVI is calculated and interpreted in vegetation detection from various remotely sensed data has made it a popular spectral vegetation index[34,35] for studying vegetation[1] and land-cover change.[36,37] For all six dates, TM NIR (B4) and Red (B3) were used to calculate NDVI using: $\mathrm{NDVI} = (\mathrm{B4} - \mathrm{B3})/(\mathrm{B4} + \mathrm{B3})$.

3.3.2 *Tasseled cap transformation*

The TC transformation[38] is a method for enhancing the spectral information content of TM data and optimizing data viewing capability in vegetation studies.[16] It was calculated for each scene using six TM bands (1 through 5 and 7).[39] The TC index fitted a linear transformation to the six TM bands using a set of empirically derived coefficients,[38] and the information present in the six original bands was compressed into three TC transformed bands: TC1 (brightness, measure of soil), TC2 (greenness, measure of vegetation), and TC3 (wetness, relationship between soil and

canopy moisture). A large amount of image variability was expressed in these three bands and was related to physical scene characteristics.[38] Greenness is a contrast between near-infrared and visible reflectance and is thus a measure of the presence and density of green vegetation.

3.4 *Land-Cover Classification*

3.4.1 *Supervised classification*

Land-cover classification was carried out on the original B1, B2, B3, and B4 (B1-4) band combination for all seasons. A supervised approach to image classification was used for LULC mapping and comparison of classification accuracy. The classification was performed through (1) identification of features and selection of training areas; (2) evaluation and analysis of training signature statistics and spectral patterns; and (3) classification of the images. Preliminary reference points were randomly selected for all identified LULC classes through on-screen digitization based on information obtained from topographical maps (1:250000) and the digital land-use map for the year 2000 for eastern NSW (1:100000). The points were then cross-checked and confirmed through GPS-based field surveys conducted in March (2009), May (2009 and 2011), September (2009), and November (2010). Care was taken to keep only those points that remained unchanged during the 2007 to 2009 periods. The points were also modified for classes such as crop and fallow and also for dense and low-medium density improved pasture, depending upon their condition in various seasons. These sample points were used to create sample polygons of 3×3, 5×5, or 7×7 pixels depending on the class homogeneity. A total of 696 sample polygons, giving an average of 77 samples per class, were collected for all land-cover classes based on stratified random sampling to include all defined land-cover types in the region. From the total sample of polygons, 132 training polygons (about 10 to 16 polygons per class) were randomly selected for signature generation and classification. Signatures were further refined based on separability analysis in terms of Jeffries–Matusita (JM) distance and Transformed Divergence (TD) separability measures. Supervised classification on B1-4 (supB1-4) was performed using maximum likelihood classifier (MLC).[39] Similar methods were applied for the classification of images for all dates.

3.5 *Density slicing of NDVI (DS-NDVI) and TC2 (Greenness) (DS-TC2)*

As both NDVI and TC2 are global vegetation indices that can be used to measure vegetation greenness and density,[16] an attempt was made to compare the effectiveness of two images in terms of identifying variations in vegetation density or LULC. The NDVI and TC2 images on each date were classified and then compared to identify changes. Density slicing, a pseudo-Color enhancement technique, was applied on NDVI and TC2 images of each date for LULC classification. The process was considered an effective way of highlighting different LULC classes by slicing the range of grey-scale values (0 to 255) and assigning different Colors to each of those slices.[40] A user defined look-up-table (LUT) was generated by selecting the upper and lower limits of pixel values for each class, through interactive visual inspection and ground-truthed pixels generated in supervised classification for each LULC class. The resultant color-coded classified images were exported to a GIS for seasonal LULC variation studies.

3.6 *Mapping Seasonal Variations in LULC*

3.6.1 *LULC change reference data*

The visual interpretation method of Cohen et al.[41] was used for developing reference data for LULC change identification error evaluations. Initially, change pixels were identified on the January, March, and May color composites (R:G:B; 4:5:3) and then a three-date (e.g., Jan–Mar–May) change-detection classification scheme (Table 2) was developed to identify changes between LULC classes during that period. For example, areas with existing vegetation cover are coded as "*Y*," and those with no-vegetation as "*N*" on each date, thus on three-date change scheme, YNY code implied vegetation cover to be present before or in January, harvested

Table 2 Three-Date LULC change detection scheme for the study region.

Code	Description
NCHBM	No change in high biomass
NCLMBM	No change in low-medium biomass
NCWB	No change in waterbody
NYY	Cleared before date1, regrow date1 to date2
YNY	Cleared date1 to date2, regrow date2 to date3
YYN	Cleared date2 to date3
NNY	Cleared before date1, regrow date2 to date3
NYN	Cleared before date1, regrow date1 to date2, cleared date2 to date3
YNN	Cleared date1 to date2, no regrow
NCNBM	No change in no biomass
C-VD	Change in vegetation density

Y, vegetation present; *N*, vegetation absent; e.g., YNN, vegetation present on date1, cleared between date1 & date2 and no regrowth between date2 & date3; etc.

between January and March and again re-grow between March and May. Based on field data information on each LULC class, gathered during filed visits in selected months, as explained in the supervised classification process, reference points for change evaluations process were generated for each change class. Though the reference points were selected based on previous field information, approximately 30% of the total reference points were further randomly examined during the survey conducted in different months in the 2010 to 2011 periods. The process was carefully executed and wherever required, necessary modifications or improvements were made by readjustment/discarding of any existing point or by inclusion of few additional points. For Jan., Mar., and May change, 759 sample points were selected across all change categories, from which 124 sample points were used for classification and the remaining points being used for accuracy assessment. The classification reference points were used to make reference polygons of 3×3 or 5×5 pixels for signature generation. Similarly, 694 sample points (102 for training and 592 for accuracy assessment) and 761 sample points (118 for training and 643 for accuracy assessment) were selected for two other three-date changes (May–Aug–Sept and Sept–Nov–Jan), respectively, and similar interpretations were made for identification of changes between dates.

3.7 *RGB-NDVI and RGB-TC2 Classifications*

Digital change detection was mostly carried out by comparing two images of different dates and recording the changes between them. However, the analysis of three or more date images allowed trends to be examined at more than one time interval. The visual RGB-NDVI method by Sader and Winne[21] was the most simple and effective method for change detection involving images of three or more dates. The method utilizes additive Color theory when a color composite image is created by displaying three consecutive dates NDVI image as red, green, and blue color guns, respectively. Any combination of primary colors of similar brightness produces a complementary color.[39] The method works well with cathode ray tube (CRT) and liquid crystal display (LCD) computer monitors which use phosphorous and equivalent color filters, respectively, on similar chromaticity coordinates. However, the method has limitation with light emitting diode (LED) monitors as its chromaticity coordinates typically exist outside of the color range of CRT and LCD displays.[42] By knowing the order of date of NDVI image displayed, the complementary colors reflect the changes.[21] For example, if NDVI images of three different

dates are displayed in sequence as red, green, and blue, then if a crop present in date 1 and date 2 but is harvested before date 3, it can be identified by yellow color and so on. To quantify the changes, an unsupervised classification using the ISODATA clustering algorithm was performed on each three-date NDVI dataset to generate 25 multitemporal cluster classes. These clusters were later modified and merged with the help of a defined LULC change scheme (Table 2) to generate signatures for each of the change categories. These signatures, along with the reference points generated earlier, were used in supervised classification for three-date change/no-change mapping. Similar method was applied for RGB-TC2 classification using three date TC2 images.

3.8 *GIS Integration of Classifications for LULC Change Analysis*

The classified outputs from supB1-4, DS-NDVI and DS-TC2 consisting of nine land-cover classes were exported to a GIS domain for land-cover change analysis. The changes in land-cover were determined in terms of variations in the greenness. To detect three-date changes and to minimize the number of change combinations, the classifications were simplified by merging/re-coding of categories such as improved pasture (IP) and crop land (CL) as high biomass (code = 5), evergreen forest (EF) and evergreen woodland (EW) as medium biomass (code = 4), natural pasture (NP) as low biomass (code = 3), fallow land black soil (FLBS) and fallow land grey/red soil (FLGRS) as no biomass (code = 2) and waterbody (WB) (code = 1) (see Sec. 2.2 and Table 1 for LULC descriptions). Similarly, LULC from NDVI and TC2 images were reclassified for all dates. To find the changes between January, March, and May (Jan–Mar–May), each monthly re-classified image was combined together using the grid tool in ARC/INFO GIS, similar to the method used by Mongkolsawat and Thirangon.[43] The method allowed mathematical combination of three grids resulting in 125 unique possible linear combinations depicting seasonal variations in different LULC categories. The process was important in the sense that it retained the class-code of each of the input layers in the output grid as well as assigning a unique code to each of the linear combinations in a separate field. Thus each combination could be studied separately with respect to possible changes and, when required, could be regrouped to provide a meaningful land-cover dynamic between dates. The process was repeated for determining LULC seasonal variations between May, August, and September (May–Aug–Sept) and also between September, November, and January (Sept–Nov–Jan).

3.9 *Accuracy Assessment*

3.9.1 *LULC classification and seasonal variation accuracy assessment*

The LULC classification accuracy of each image and for the three-date change images was expressed in the form of an error matrix, an array of rows and columns where rows indicate number of pixels assigned to a particular land-cover class and columns represent reference data or actual class, as verified in the field. The accuracy was expressed as producer's error (error of omission), user's error (error of inclusion or commission) and overall accuracy.[44–46] Kappa coefficient ($\hat{K}$)[44,47] was also used as a measure of classification accuracy. It has the advantage of being able to calculate a confidence interval and thus statistically comparing two or more classifications. The Kappa was computed as:

$$\hat{K} = \frac{N\sum_{i=1}^{r} x_{ii} - \sum_{i=1}^{r} x_{i+}x_{+i}}{N^2 - \sum_{i=1}^{r} x_{i+}x_{+i}},$$

where r is the number of rows in the matrix, x_{ii} is the number of observations in row i and column i (the i'th diagonal elements), x_{i+} and x_{+i} are the marginal totals of row r and column i, respectively, and N is the number of observations. The Kappa coefficient and variances of the error matrices for RGB-NDVI, RGB-TC2, supB1-4, DS-NDVI, and DS-TC2 were used in a pair-wise test of significance.[48] The Z-statistics computed in this test compared a pair of $\hat{K}$ statistics obtained from the error matrices of two classifications, to determine if they were significantly different. Z-statistics was computed as:

$$Z = \frac{K_1 - K_2}{(V_1 + V_2)^{1/2}},$$

where K_1 and K_2 are the estimated Kappa statistics for two classifications, and V_1 and V_2 are the large sample variances of the respective Kappa statistics. The Z statistics follows a normal distribution.

3.9.2 *Conditional Kappa*

An attempt was made to look at the agreement for an individual class within the classification error matrix for each date. This identified the most suitable date for a particular LULC classification by comparing its accuracies on different dates. The process was implemented through computation of a conditional Kappa ($K_{\hat{i}}$)[49] for each LULC class and conditional agreement for the i'th category was given by:

$$K_{\hat{i}} = \frac{Nx_{ii} - x_{i+}x_{+i}}{Nx_{i+} - x_{i+}x_{+i}}.$$

Here each term is as defined previously. The same comparison tests used in case of Kappa was applied to this conditional Kappa for an individual LULC class.

3.10 *Referential Refinement and Aggregation*

January, August, and November reclassified images were used to produce an overall LULC map of the region based on a process called referential refinement and aggregation.[50] Adinarayana and Krishna[51] applied per pixel logical combinations on monsoon and post-monsoon classifications to discriminate different types of LULC classes in India. The unique feature of this method is that it allows human logic and perception to modify a classification. In referential refinement, classification of a pixel in one season was evaluated and, if necessary, corrected or modified with respect to the corresponding pixel class in the other season. For example, a pixel classified as a crop both in January and August images was termed "double cropped" in the aggregate map. Similarly, a pixel under crop in January but fallow in August was termed a "single crop" or "summer crop" area. Table 3 summarizes the logical combinations applied in the aggregation process taking the January classification as a reference. The process was further extended by combining a third November (late spring) classification to mainly distinguish C3 and C4 dominated pastures in the area.[27] March and May classification results were not found much useful in discrimination of C3 and C4 pastures, a dominant land-cover category in the area. The use of spring data in pasture mapping in northern tablelands of NSW was also recommended by Hill et al.[27] Peterson et al.[14] also found that spring and summer season data was useful to discriminate summer and winter-active grasses in northeastern Kansas, USA, but not fall data.

3.11 *LULC Classification in Summers of Different Years*

Since LULC and vegetation respond differently to inter-annual variability in rainfall and temperature,[52,53] we verified whether the results obtained from single-date imagery applied in other years. To begin with, summer (October to January) rainfall was computed for the period 1990 to 2010 for 20 different stations in the region to identify years of high rainfall (wet), normal rainfall, and low rainfall (drought) (Fig. 3). The summers of 2004, 2007, and 2010 were identified as wet, drought, and normal, respectively. Since January 2007 (dry summer) was analyzed previously, two additional satellite images (February 2004, February 2010) were processed and classified as described earlier. No cloud-free data for January in the two selected years were available; therefore imagery from the next closest available date was used. The classification accuracies obtained with B1-4 (supB1-4) were compared with previous results.

To use available reference data from recent years for the classification and accuracy evaluation of 2004 image, additional processing was done to include only those points that had not

Table 3 Logical aggregation of January, August, and November classifications to generate aggregate LULC map.[27]

Aggregate class description	NDVI profile with respect to season	Location element	Aggregate code
Sown perennial pasture dominated by summer grasses with some woodland	Extended peak in spring and summer (NDVI high in Nov and Jan and low in Aug)	High elevation sown perennial pastures	IP (C4)
Seasonal perennial grasses dominated by winter grasses with annual legumes	Spring peak, decays quickly in late spring (NDVI low in Jan and high in Aug & Nov)	On slope adjacent to tablelands	IP (C3)
Sown perennial pastures with high woodland/forest content, mixed with both winter and summer grasses	(a) High NDVI all year, extended spring NDVI value (b) High NDVI value with some seasonality, high summer value	On high elevation and on eastern escarpments at high elevation	Mixed IP (C3 & C4)
Native pasture woodland dominated by summer grasses	High summer NDVI (high in Jan, low in Aug and Nov)	On north of New England range and on eastern edge of northern tablelands	NP(C4)
Improved native with minimal woodlands	Seasonal NDVI low in summer (high in Nov & Aug and low in Jan)	On northern slopes	NP (C3)
Native pasture and woodland	High summer and Autumn/ winter NDVI (high in Jan and Aug)	On eastern edge throughout northern tablelands	Mixed NP (C3 &C4)
Dryland crops, fallow and some pastures (crop rotations, short term forage and lucerne	Seasonal NDVI (high in Jan, low in Aug & Nov and vice versa)	High elevation and along the slopes adjacent to tablelands	Mixed (pasture/crop)
Summer crops (e.g., cotton)	High spring and summer NDVI (high in Jan and Nov, low in Aug)	South-western part of the region	SC
Wintyr crops (e.g., wheat)	High autumn and winter NDVI, low in spring/ summer (high in Aug, low in Nov & Jan)	Northern and south-west part of the region	WC
Double crops (both summer and winter seasons were used for crop production)	Seasonal NDVI (high in Jan, Aug and Nov)	Northern and south-west part of the region	DC
Double Fallow (not used for any agricultural activity in any season)	Low seasonal NDVI (Jan, Aug and Nov)	Scattered in the region	DF
Evergreen forest	High/medium NDVI throughout the year (Jan, Aug and Nov)	Scattered in the region	EF
Evergreen woodland	Medium to low NDVI throughout the year (Jan, Aug and Nov)	Scattered in the region	EW
Waterbody	Very low NDVI throughout the year (Jan, Aug and Nov)	Scattered in the region	WB

changed during these periods. A change/no-change image was created from 2004 to 2007 difference image using ± 1 standard deviation (SD) as a threshold.[30] All 2009 to 2010 validation points were assessed in comparison to the change images and sites that fell on areas greater than ± 1 SD from the mean were discarded. The remaining sites were assumed to have not changed

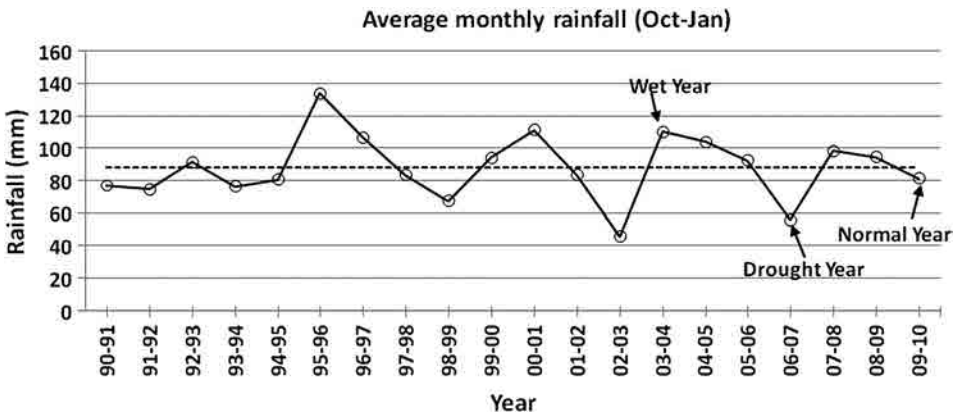

Fig. 3 Average rainfall (October to January) from 1990 to 2010 in the study region for the identification of high, normal, and low rainfall years.

over the years and were used as validation data for classifications. Finally, McNemar's test[54] was used by computing the chi-square (χ^2) statistic on one degree of freedom[55] to compare the overall accuracies for summer data in three different rainfall conditions.

4 Results and Discussion

4.1 *LULC Classification*

Table 4 shows LULC class accuracies in terms of producer, user, overall and Kappa coefficients for all months with supB1-4 by comparing the location and class of each ground-truthed pixel with the corresponding location and class in the classification images. From the supB1-4 classifications, the highest overall accuracy was achieved with the January image (96.7%,

Table 4 LULC classification accuracies using the supB1-4 combination in each month obtained by comparing the classifications with reference data (see Table 1 for LULC descriptions).

	Jan		Mar		May		Aug		Sept		Nov	
LULC Class	Prod.	User	Prod.	User	Prod.	User	Prod.	User	Prod.	User	Prod.	User
EF	71.3	100.0	83.5	98.6	100.0	98.8	71.0	98.4	82.3	100.0	83.3	100.0
EW	100.0	74.1	99.3	84.4	99.8	96.3	98.5	72.4	100.0	82.0	100.0	86.1
IP-HD	99.4	100.0	82.0	79.7	85.3	95.8	84.3	51.0	96.4	77.8	94.7	97.8
IP-LMD	98.8	100.0	77.3	64.5	94.6	89.1	96.3	87.9	79.7	99.5	99.7	93.7
CL	100.0	99.6	85.5	100.0	96.5	85.6	61.6	99.1	60.0	100.0	97.7	93.7
FLBS	100.0	100.0	100.0	99.5	94.4	99.6	99.8	95.4	84.3	100.0	99.8	80.8
FLGRS	100.0	100.0	99.1	100.0	98.8	100.0	91.4	100.0	97.0	65.6	55.1	100.0
NP	100.0	99.3	88.1	86.7	100.0	97.7	97.6	92.2	100.0	53.3	97.4	100.0
WB	100.0	100.0	100.0	100.0	100.0	100.0	87.5	100.0	100.0	100.0	100.0	100.0
Overall Accuracy	**96.7%**		**91.1%**		**96.0%**		**86.9%**		**85.7%**		**93.9%**	
Kappa Coefficient	**0.96**		**0.90**		**0.95**		**0.85**		**0.83**		**0.93**	

Prod. = Producer Accuracy, User = User Accuracy.
EF, evergreen forest; EW, evergreen woodland; NP, native pasture, IP-HD, improved pasture-high density; IP-LMD, improved pasture-low medium density; CL, crop land; FLBS, fallow land-black soil; FLGRS, fallow land grey/red soil; and WB, waterbody.

Kappa = 0.96), while it was much lower in the case of the August (86.9%, Kappa = 0.85) and September (85.7%, Kappa = 0.83) images (Table 4).

In the case of the January image, almost all of the LULC classes were spectrally separable producing high classification accuracies, except for intermixing of the evergreen forest (EF) and evergreen woodland (EW) categories. Although confusion between crop land (CL), improved pasture low and medium density (IP-LMD), improved pasture high density (IP-HD) and natural pasture (NP), and between EF and EW was observed in all months, the former set was particularly difficult to distinguish in August and September due to high intermixing between these classes. EF and EW were most confused in January. The reasons for high spectral mixing between different types of grasslands (native and introduced) and crops in late winter and early spring was attributed to the similar spectral responses of winter-active plants in crops, sown, native, and naturalized pastures, and grasslands in early spring. However, the confusion diminished in late spring and mid-summer when winter-active grasses had died or were diminished and summer-active grasses were in peak growth in native and naturalized pastures, thus were clearly differentiable from the stubble of C3 crops, sown C3 pastures, which were less active in mid-summer and C4 crops. Table 5 shows the $K_{\hat{i}}$ computed for individual classes for all dates and corresponding Z-values for the classes when $K_{\hat{i}}$ was less than 1. The values reflect the relative accuracy obtained for each class on different dates.

Category EF was classified correctly ($K_{\hat{i}} = 1$) in January, September, and November months, while it was marginally less accurately classified in other months. These patterns indicated that class EF could be mapped from any of the selected dates without spectral confusion with remaining LULC classes. In the case of EW, none of the dates showed full agreement in classification accuracy, May ($K_{\hat{i}} = 0.96$) being the highest, followed by November and March, while agreement in January was the least ($K_{\hat{i}} = 0.72$). Therefore, May was the best period for EW classification. The two types of grazed pasture (IP-HD and IP-LMD) were classified correctly 100% of the time in January, with marginally lower agreement in September and November. Since the region is characterized by both summer and winter-active plants with different phenological cycles, vegetation dominated by plants with the two biochemical pathways was easily separable in early and late spring and summer, and hence September to January was the best period for their mapping. As summer and winter crops are grown in different seasons, the CL category in one season should not be compared with another. However, considering $K_{\hat{i}}$ values, this class in most months has showed 100% agreement with the classification error matrix, except in May and November. Fallow land with black and grey/red soil conditions (FLBS and FLGRS, respectively) were also in high accord with the error matrices in most of the months, except November for FLBS and September for FLGRS. Natural grazing land (NP) had showed highest $K_{\hat{i}}$ in November, followed by January, and hence these two months were considered the best for their classification. Water bodies (WB) had 100% classification agreement at all dates.

Table 5 Conditional Kappa ($K_{\hat{i}}$) of each LULC class in different months and corresponding Z-values for the classes when $K_{\hat{i}}$ was less than 1. The values reflect the relative accuracy obtained for each class on different dates. Value approaching 1 indicates higher accuracy.

Month/LULC class	EF	EW	IP-HD	IP-LMD	CL	FLBS	FLGRS	NP	WB
Jan	1.00	0.72	1.00	1.00	1.00	1.00	1.00	0.99	1.00
Mar	0.98	0.83	0.78	0.61	1.00	1.00	1.00	0.84	1.00
May	0.99	0.96	0.95	0.88	0.85	1.00	1.00	0.97	1.00
Aug	0.98	0.70	0.61	0.57	1.00	0.94	0.98	0.97	1.00
Sept	1.00	0.81	0.76	0.99	1.00	1.00	0.63	0.49	1.00
Nov	1.00	0.85	0.98	0.93	0.93	0.78	1.00	1.00	1.00

EF, evergreen forest; EW, evergreen woodland; NP, native pasture; IP-HD, improved pasture-high density; IP-LMD, improved pasture-low medium density; CL, crop land; FLBS, fallow land-black soil; FLGRS, fallow land grey/red soil; and WB, waterbody.

Table 6 Z-statistics for comparison of the conditional Kappa K_i of each LULC class taking January as a reference and comparing the corresponding LULC class in other months (see Table 1 for LULC description).

LULC		LULC					
Jan (reference)			Mar	May	Aug	Sept	Nov
EF		EF	2.83[a]	1.81(NS)	3.2[a]	—	—
EW		EW	3.36[b]	8.08[b]	0.58(NS)	2.75[a]	3.98[b]
IP-HD		IP-HD	11.19[b]	5.55[b]	18.88[b]	15.6[b]	2.61[a]
IP-LMD	VERSUS	IP-LMD	18.87[b]	8.26[b]	26.4[b]	3.35[b]	5.85[b]
CL		CL	—	19.37[b]	—	—	5.18[b]
FLBS		FLBS			7.72[b]	—	15.72[b]
FLGRS		FLGRS			2.51[a]	20.75[b]	—
NP		NP	11.47[b]	2.41[a]	NS	35.3[b]	2.8[a]
WB		WB	—	—	—	—	—

[a]Significant at 97.5% confidence level;
[b]Significant at 99.9% confidence level;
NS, not significant at 95% confidence level.
EF, evergreen forest; EW, evergreen woodland; NP, native pasture; IP-HD, improved pasture-high density; IP-LMD, improved pasture-low medium density; CL, crop land; FLBS, fallow land-black soil; FLGRS, fallow land grey/red soil; and WB, waterbody.

The above interpretations were found useful in deciding the most suitable period for mapping a particular LULC category (e.g., CL or NP etc.) in the region. Most of the LULC classes showed highest K_i with the January classification, except for EW category. January also achieved the highest overall classification accuracy (96.7%, Kappa = 0.96). Thus January was the best month for LULC classification in the region, except for EW for which May was best. This interpretation was supported by pair-wise tests of significance using for each class pair (Table 6) and was also explained by Sinha et al.[56] The Z-statistics showed that each class determined from January classifications differed significantly from the corresponding class in other months at the 99.9% confidence level in most cases.

The most suitable (January) season was examined further with respect to their utility for LULC classification in different years and under different environmental conditions in order to test the conclusion based on data from just a single year. The overall classification accuracies for wet (2004), dry (2007), and normal (2010) rainfall summers with the B1-4 band combination were 96.0%, 96.7%, and 96.9%, respectively. The results corroborated the previous observations about the greater suitability of summer for land-cover classification in the region as comparable results were obtained under all rainfall conditions (wet, drought, and normal). McNemar's test results (χ^2) computed based on number of pixels correctly and incorrectly classified in three summers further confirmed that the three results did not differ significantly under all rainfall conditions ($P < 0.001$).

4.2 *Seasonal Variations in LULC*

Figure 4 shows the comparison of overall accuracies of LULC class change for three three-date composites (Jan–Mar–May, May–Aug–Sept, and Sept–Nov–Jan) using the five methods. Kappa statistics and variances computed from change error matrices for each method were used to determine if the agreement between changes and the reference data were significantly greater than 0 (i.e., better than a random change classification if the resultant Z-value > 1.96 at 95% confidence level). The performances of RGB-NDVI, RBG-TC2, and supB1-4 were found better than DS-NDVI and DS-TC2. Higher accuracies were obtained with RGB-NDVI than with the

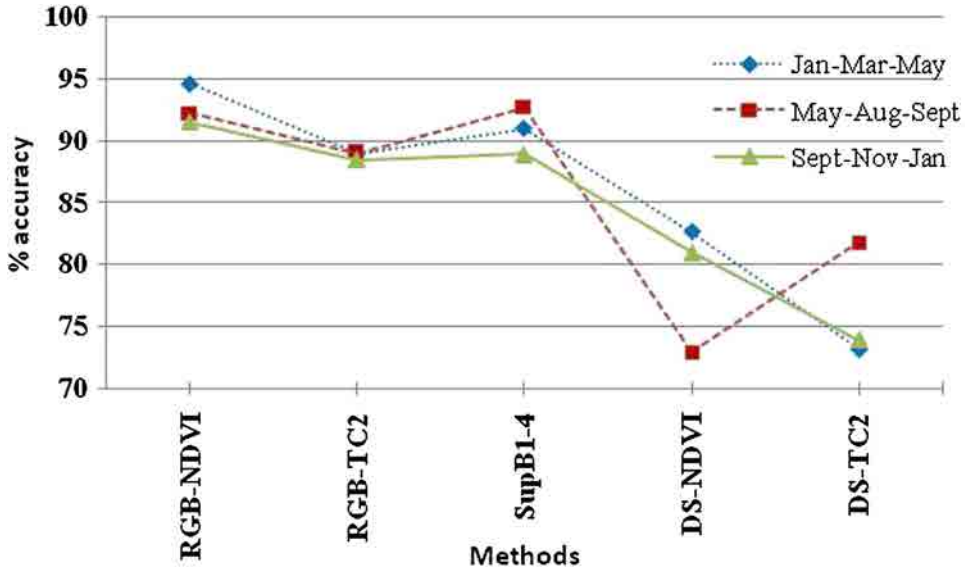

Fig. 4 Comparison of overall accuracy in LULC class change with different methods and three date composites.

other methods in each three-date composite. The highest accuracy of 94.6% (Kappa = 0.93) was obtained in the case of the Jan–Mar–May composite by this method. The supB-4 method was second best in identifying changes with overall accuracy ranging from 92.7% (Kappa = 0.91) in May–Aug–Sept to 91.0% (Kappa = 0.89) in Jan–Mar–May, and 88.9% (Kappa = 0.87) in Sept–Nov–Jan. The performance of RGB-TC2 was inferior to that of supB1-4, but much superior to that of the DS-NDVI and DS-TC2 methods. DS-TC2 was the least successful approach in all three-date composites with an overall accuracy of 73.2% (Kappa = 0.7), 81.8% (Kappa = 0.8), and 74% (Kappa = 0.71), respectively. In general, the user's and producer's accuracies of certain LULC change classes, such as YNY and NYN, with all three-date composites were lower than change classes, NYY, YYN, NNY, and YNN, regardless of method used (here *Y* and *N* stand for vegetation present and absent on any date, respectively). For example, YNY code implied vegetation cover to be present before or on date1, harvested between date1 and date2 and again re-grow between date2 and date3; refer to Table 2 for description). Higher accuracies were obtained for change class containing two similar LULC classes, vegetation or nonvegetation, on two sequential dates (e.g., YYN or NNY), as compared to class containing alternative vegetation and nonvegetation categories on two sequential dates (e.g., NYN or YNY). High accuracies were also obtained with all date composites in the case of the no-change categories (no change in high biomass (NCHBM), no change in low medium biomass (NCLMBM), No change in waterbody (NCWB), and no change in no biomass (NCNBM), and change in vegetation density (C-VD) (see Table 2 for class description), where three similar LULC classes on three sequential dates were present.

The RGB-NDVI results were compared with each of the other methods for all the three-date composites. The *Z*-statistics computed for each comparison in each season are summarized in Table 7. The RGB-NDVI methods were significantly different from the other methods for all dates at the 99.9% confidence level, except for RGB-TC2 and supB1-4 with the May–Aug–Sept composite. RGB-NDVI was best for identifying seasonal variation in the region, and the results obtained with it were selected for further discussion and were used for seasonal variation mapping.

Table 8 shows percent area LULC changes for each three-date composite using RGB-NDVI and Fig. 5 shows a LULC seasonal variation map of parts of the study region using three-date-composites of different periods. Nearly 14% of NCHBM and 13% of NCNBM categories did not exhibit any changes between January and May. However, the region experienced major changes in NYY (32%) and in C-VD (32%) during this period, mostly due to winter-active pastures, which often become active and restart growth in autumn. Nearly 50% of the region did not experience any change between May to September in vegetated or nonvegetated areas. However,

Table 7 Test statistic (Z) for pair-wise comparison of RGB-NDVI with respect to other methods.

Comparison	Jan–Mar–May	May–Aug–Sept	Sept–Nov–Jan
RGB-NDVI vs RGB-TC2	5.23[a]	1.07(NS)	4.57[a]
RGB-NDVI vs supB1-4	4.46[a]	0.3(NS)	4.06[a]
RGB-NDVI vs DS-NDVI	7.35[a]	8.33[a]	9.58[a]
RGB-NDVI vs DS-TC2	11.23[a]	5.58[a]	13.05[a]

changes in NYY, YNY, and NNY, comprising nearly 16% of the region, were mostly due to growth of winter-active C3 pastures in early to late spring. One of the major changes (nearly 29%) in the region during this period was in the YYN category; mainly due to winter crop production, sown in autumn and harvested in late spring. The 4% change in YNN was mainly due to autumn C3 pastures, but no significant change in vegetation density was observed between these periods. Nearly 17% of the region experienced no change in the high biomass category (NCHBM) between September and January (Sept–Nov–Jan composite), mostly due to summer-active C4 pastures, which have a growth period from spring until mid summer. However, nearly 18% of the region was devoid of any vegetation cover during this period. The changes observed in YNY (~7%), YYN (~40%), NNY (~4%) and YNN (~8.5%) were mostly due to the presence of improved or natural pastures with varying phenologies and level of growth activity and dormancy.

4.3 *LULC Aggregation*

The LULC area statistics generated from the aggregate map (Fig. 6) showed evergreen woodland (EW) to be the dominant category in the region, covering nearly 54% of the total area. These

Table 8 Percent area of LULC change for each of the three-date composites using RGB-NDVI method.

LULC change	Area (%)Jan–Mar–May	Area (%)May–Aug–Sept	Area (%)Sept–Nov–Jan
NCHBM	14.09	0.65	17.32
NCLMBM	NS	47.66	NS
NCWB	NS	NS	0.40
NYY	32.31	2.74	0.44
YNY	0.83	12.52	6.82
YYN	0.18	28.89	39.65
NNY	3.41	1.11	3.83
NYN	1.03	0.41	4.68
YNN	2.48	4.21	8.49
NCNBM	13.11	1.81	18.35
C-VD	32.55	NS	NS

NS, not significant.
NCHBM, no change in high biomass; NCLMBM, no change in low-medium biomass; NCWB, no change in waterbody; NCNBM, no change in no biomass; C-VD, change in vegetation density; *Y*, vegetation present; *N*, vegetation absent; e.g., YNN, vegetation present on date1, cleared between date1 & date2 and no regrowth between date2 & date3; etc.

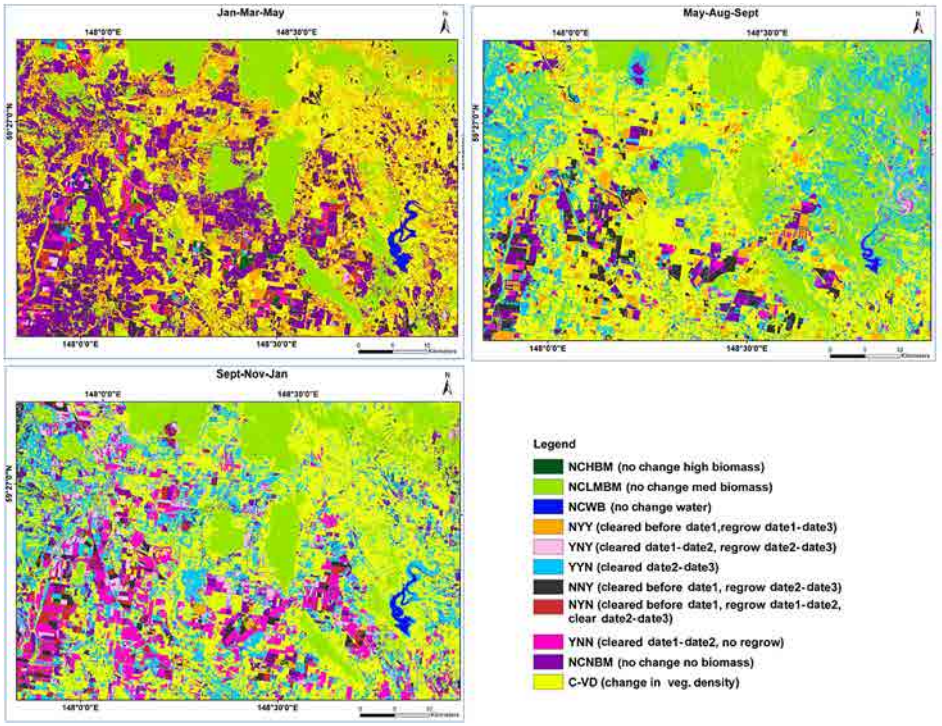

Fig. 5 Seasonal variation in LULC using the RGB-NDVI method in Jan–Mar–May, May–Aug–Sept, and Sept–Nov–Jan composites.

areas were characterized by low to medium tree density, mostly on rugged steep rocky hills and peaks, and consisted of snow gum and manna gum on the highest points with silver-topped stringybark, broad-leaved stringybark, and red stringybark. Black cypress pine and white cypress pine mostly occurred on steep slopes while yellow box and white box are predominated on lower slopes.[57] The second most important category identified in the region was improved C4 grazing pasture (sown) occupying nearly 25% of the study region, mostly used for livestock production. This LULC category may be part of crop–pasture rotations.

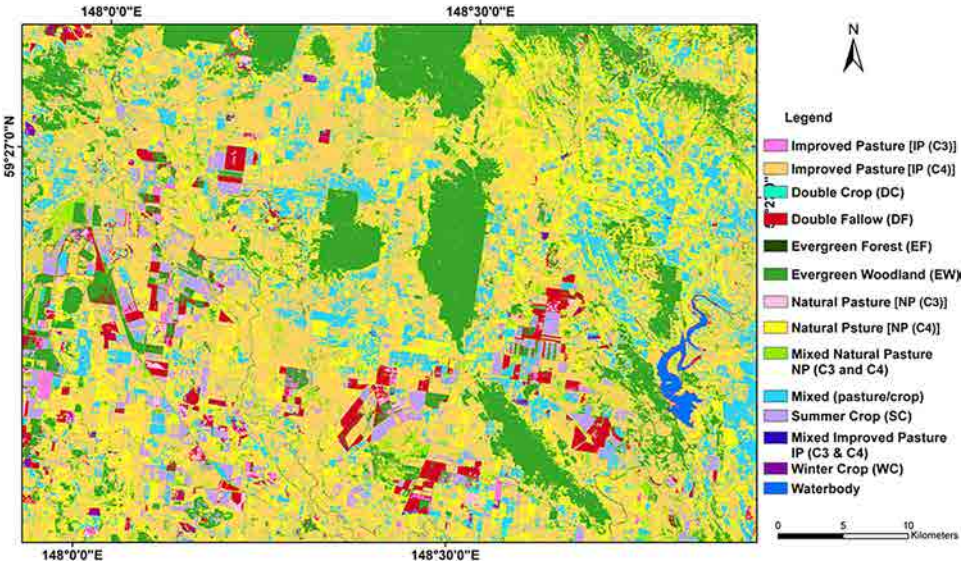

Fig. 6 LULC aggregate map of a part of the study region generated by aggregating January, August, and November classifications and referential refinement processes (refer to Table 3 for class code descriptions).

Native pasture (dominated by C4 grasses) was another major category identified in the region, covering nearly 9% of the total area. Therefore, both categories of grazed pastures, natural and sown, dominated the region. Mixed pasture types and also mixed crop and pasture were identified in 8% of the region. The remaining LULC categories were found over 3% of the region. The aggregate output clearly provided a means for understanding the overall land use distribution of the region. The major land uses in the region were grazing pasture production, from both native and sown pastures, and also crop and pasture production as a part of crop–pasture rotations.

5 Conclusions

Analysis of sequential date Landsat TM images determined January (summer) to be the best month in terms of overall accuracy in LULC classification as classes were spectrally more distinguishable compared to other dates. This was confirmed using conditional Kappa (K_i) coefficient with most classes showing 100% agreement with the January classification. The analysis of additional summer images under different rainfall (wet, drought and normal) conditions further confirmed the superiority of land-cover classification during January (summer). Three-date seasonal changes in various LULC categories were most correctly identified using RGB-NDVI compared with NDVI-TC2, supB1-4, DS-NDVI and DS-TC2 methods. The aggregate output clearly provided a means for understanding overall land-use distribution in the region. The major activities identified in the region were livestock production from grazed pastures, both natural and sown, and crop and pasture production as a part of crop–pasture rotation system.

The study demonstrated the potential of remote sensing and GIS in LULC mapping and identifying seasonal dynamics in a region with complex changes in both summer and winter LULC. The use of six sequential date images for LULC seasonal variation mapping made this study unique from traditional change-detection studies, where changes are identified mostly from two or three images of nonsequential dates. The research highlighted the usefulness of multiseasonal data in better understanding the spectral response of each of the LULC classes and their extent of inter-mixing in different seasons. This in turn provided scope for the user in deciding the best date and image for classification of an individual LULC category in a given year. Use of sequential date images provided more flexibility in the selection of second or third-best alternative periods in mapping a particular LULC, in case of constraint such as cloud cover over the target class during the best period. Further, use of three-date composites offered a better way of understanding LULC practices in the region and also helped in identifying classes with different phenology. The referential refinement and aggregation processes used here provided a means for understanding the level of land exploitation (extensive versus intensive) activities carried out in the region. The process not only helped in the identification of classes under cloud in one season but also provided annual estimates of land-use in the region.

References

1. Bureau of Rural science (BRS), "Guidelines for land use mapping in Australia: principles, procedures and definitions," in *A technical handbook supporting the Australian Collaborative Land Use Mapping Programme*, 3rd ed., BRS Publication Sales, Canberra ACT (2006), http://adl.brs.gov.au/data/warehouse/aclump9abc_007/aclump9abc_00711a08/landUseMappingAustGuidelines_ed3.pdf.
2. R. J. Hobbs, "Effects of landscape fragmentation on ecosystem processes in the Western Australian wheatbel," *Biol. Conserv.* **64**(3), 193–201 (1993), http://dx.doi.org/10.1016/0006-3207(93)90321-Q.
3. R. S. Reid et al., "Land-use and land-cover dynamics in response to change in climatic, biological and socio-political forces: the case of southwestern Ethiopia," *Landscape Ecol.* **15**(4) 339–355 (2000), http://dx.doi.org/10.1023/A:1008177712995.
4. A. De Sherbinin, "A CIESIN thematic guide to Land-Use and Land-Cover Change (LUCC)," Center for Intern. Earth Science Information Network (CIESIN) Columbia University Palisades, NY, USA, (2002), http://sedac. ciesin. columbia. edu/guides/lu/CIESIN_LUCC_TG. Pdf.

5. C. Xiuwan, "Using remote sensing and GIS to analyse land cover change and its impacts on regional sustainable development," *Int. J. Rem. Sens.* **23**(1), 107–124 (2002), http://dx.doi.org/10.1080/01431160010007051.
6. A. Falcucci, L. Maiorano, and L. Boitani, "Changes in land-use/land-cover patterns in Italy and their implications for biodiversity conservation," *Landscape Ecol.* **22**(4), 617–631 (2007), http://dx.doi.org/10.1007/s10980-006-9056-4.
7. P. Coppin et al., "Digital change detection methods in ecosystem monitoring, a review," *Int. J. Rem. Sens.* **25**(9), 1565–1596 (2004), http://dx.doi.org/10.1080/0143116031000101675.
8. M. Pax-Lenney and C. E. Woodcock, "Monitoring agricultural lands in Egypt with multitemporal landsat TM imagery: how many images are needed?," *Rem. Sens. Environ.* **59**(3), 522–529 (1997), http://dx.doi.org/10.1016/S0034-4257(96)00124-1.
9. B. C. Reed et al., "Measuring phenological variability from satellite imagery," *J. Vegetat. Sci.* **5**(5), 703–714 (1994), http://dx.doi.org/10.2307/3235884.
10. J. R. Schriever and R. G. Congalton, "Evaluating seasonal variability as an aid to cover-type mapping from landsat thematic mapper data in the Northeast," *Photogramm. Eng. Rem. Sens.* **61**(3), 321–327 (1995).
11. P. T. Wolter et al., "Improved forest classification in the northern lakes states using multitemporal landsat imagery," *Photogramm. Eng. Rem. Sens.* **61**(9), 1129–1143(1995).
12. T. Murakami, "Seasonal variation in classification accuracy of forest-cover types examined by a single band or band combinations," *J. Forest Res.* **9**, 211–215 (2004), http://dx.doi.org/10.1007/s10310-004-0075-1.
13. E. H. Wilson and S. A. Sader, "Detection of forest harvest type using multiple dates of landsat TM imagery," *Rem. Sens. Environ.* **80**(3), 385–396 (2002), http://dx.doi.org/10.1016/S0034-4257(01)00318-2.
14. D. Peterson, K. Price, and E. Martinko, "Discriminating between cool season and warm season grassland cover types in northeastern Kansas," *Int. J. Rem. Sens.* **23**(23), 5015–5030 (2002), http://dx.doi.org/10.1080/01431160210142833.
15. K. Green, D. Kempka, and L. Lackey, "Using Re. Sens. to detect and monitor land-cover and land-use change," *Photogramm. Eng. Rem. Sens.* **60**(3), 331–337 (1994).
16. J. Jensen, *Introductory Digital Image Processing: A Remote Sensing Perspective*, Pearson Prentice Hall, Upper Saddle River, NJ (2005).
17. D. Lu et al., "Change detection techniques," *Int. J. Rem. Sens.* **25**(12), 2365–2407 (2004), http://dx.doi.org/10.1080/0143116031000139863.
18. A. Miller, E. Bryant, and R. Birnie, "An analysis of land cover changes in the Northern forest of New England using multitemporal landsat MSS data," *Int. J. Rem. Sens.* **19**(2), 245–265 (1998), http://dx.doi.org/10.1080/014311698216233.
19. L. Muñoz-Villers and J. López-Blanco, "Land use/cover changes using landsat TM/ETM images in a tropical and biodiverse mountainous area of central-eastern Mexico," *Int. J. Rem. Sens.* **29**(1), 71–93 (2008), http://dx.doi.org/10.1080/01431160701280967.
20. M. Torres-Vera, R. Prol-Ledesma, and D. Garcia-Lopez, "Three decades of land use variations in Mexico city," *Int. J. Rem. Sens.* **30**(1), 117–138 (2009), http://dx.doi.org/10.1080/01431160802261163.
21. S. Sader and J. Winne, "RGB-NDVI color composites for visualizing forest change dynamics," *Int. J. Rem. Sens.* **13**(16), 3055–3067 (1992), http://dx.doi.org/10.1080/01431169208904102.
22. S. A. Sader et al., "Forest change monitoring of a remote—biosphere reserve," *Int. J. Rem. Sens.* **22**(10), 1937–1950 (2001), http://dx.doi.org/10.1080/01431160117141.
23. D. J. Hayes and S. A. Sader, "Comparison of change-detection techniques for monitoring tropical forest clearing and vegetation regrowth in a time series," *Photogramm. Eng. Rem. Sens.* **67**(9), 1067–1075 (2001).
24. DECC Report, "The Bioregions of New South Wales-their biodiversity, conservation and history," Department of Environ. and Climate Change, New South Wales, (2008), http://www.environment.nsw.gov.au/bioregions/BioregionOverviews.htm (accessed August 2012).
25. BoM, "Bureau of Meteorology Australia," (2010), http://www.bom.gov.au/nsw/ (accessed March 2012).

26. J. T. Baxter and L. D. Russell, "Land use mapping requirements for natural resource management in the Murray-Darling basin," Project M305: Task 6. Department of Conservation and Natural Resources, Vicoria (1994).
27. M. J. Hill et al., "Pasture land cover in eastern Australia from NOAA-AVHRR NDVI and classified Landsat TM," *Rem. Sens. Environ.* **67**(1), 32–50 (1999), http://dx.doi.org/10.1016/S0034-4257(98)00075-3.
28. G. Chander and B. Markham, "Revised Landsat-5 TM radiometric calibration procedures and postcalibration dynamic ranges," *IEEE Trans. Geosci. Rem. Sens.* **41**(11), 2674–2677 (2003), http://dx.doi.org/10.1109/TGRS.2003.818464.
29. J. C. Price, "Calibration of satellite radiometers and the comparison of vegetation indices" *Rem. Sens. Environ.* **21**(1), 15–27 (1987), http://dx.doi.org/10.1016/0034-4257(87)90003-4.
30. J. Mas, "Monitoring land-cover changes: a comparison of change detection techniques," *Int. J. Rem. Sens.* **20**(1), 139–152 (1999), http://dx.doi.org/10.1080/014311699213659.
31. D. Eckhardt, J. Verdin, and G. Lyford, "Automated update of an irrigated lands GIS using SPOT HRV imagery," *Photogrammm Eng. Rem. Sens.* **56**(11), 1515–1522 (1990).
32. J. R. Jensen et al., "Inland wetland change detection in the everglades water conservation area 2A using a time series of normalized remotely sensed data," *Photogrammm Eng. Rem. Sens.* **61**(2), 199–209 (1995).
33. M. F. Jasinski, "Sensitivity of the normalized difference vegetation index to subpixel canopy cover, soil albedo, and pixel scale," *Rem. Sens. Environ.* **32**(2–3), 169–187 (1990), http://dx.doi.org/10.1016/0034-4257(90)90016-F.
34. B. C. Gao, "NDWI—a normalized difference water index for Re. Sens. of vegetation liquid water from space," *Rem. Sens. Environ.* **58**(3), 257–266 (1996), http://dx.doi.org/10.1016/S0034-4257(96)00067-3.
35. R. Myneni and G. Asrar, "Atmospheric effects and spectral vegetation indices," *Rem. Sens. Environ.* **47**(3), 390–402 (1994), http://dx.doi.org/10.1016/0034-4257(94)90106-6.
36. T. Fung and W. Siu, "Environmental quality and its changes, an analysis using NDVI," *Intern. J. Rem. Sens.* **21**(5), 1011–1024 (2000), http://dx.doi.org/10.1080/014311600210407.
37. R. S. Lunetta et al., "Impacts of vegetation dynamics on the identification of land–cover change in a biologically complex community in North Carolina, USA," *Rem. Sens. Environ.* **82**(2–3), 258–270 (2002), http://dx.doi.org/10.1016/S0034-4257(02)00042-1.
38. E. P. Crist and R. C. Cicone, "Application of the tasseled cap concept to simulated thematic mapper data (transformation for MSS crop and soil imagery)," *Photogrammm Eng. Rem. Sens.* **50**(3), 343–352 (1984).
39. T. M. Lillesand and R. Keifer, Remote sensing and data interpretation, pp. 550–580, John Wiley and Sons, New York (1994).
40. A. Knight, D. Tindall, and B. Wilson, "A multitemporal multiple density slice method for wetland mapping across the state of Queensland, Australia," *Int. J. Rem. Sens.* **30**(13), 3365–3392 (2009), http://dx.doi.org/10.1080/01431160802562180.
41. W. B. Cohen et al., "An efficient and accurate method for mapping forest clearcuts in the Pacific Northwest using landsat imagery," *Photogrammm Eng. Rem. Sens.* **64**(4), 293–300 (1998).
42. I. Ashdown, "Accurate modeling of LED colors: a scientific approach," *LED's Magazine*, 21–23 (2005), http://www.helios32.com/LEDOctMODELING21-23_Reprint.pdf.
43. C. Mongkolsawat and P. Thirangoon, "Land cover change detection using digital analysis of remotely sensed satellite data: a methodological stud," *ACRS* (2003).
44. R. G. Congalton, R. G. Oderwald, and R. A. Mead, "Assessing landsat classification accuracy using discrete multivariate analysis statistical technique," *Photogrammm Eng. Rem. Sens.* **49**(12), 1671–1678 (1983).
45. R. G. Congalton, " A review of assessing the accuracy of classifications of remotely sensed data," *Rem. Sens. Environ.* **37**(1), 35–46 (1991), http://dx.doi.org/10.1016/0034-4257(91)90048-B.
46. P. Smits, S. Dellepiane, and R. Schowengerdt, "Quality assessment of image classification algorithms for land-cover mapping: a review and a proposal for a cost-based approach," *Int. J. Rem. Sens.* **20**(8), 1461–1486 (1999), http://dx.doi.org/10.1080/014311699212560.

47. J. Cohen, "A coefficient of agreement for nominal scales," *Educat. Psychol. Meas.* **20**, 37–46 (1960), http://dx.doi.org/10.1177/001316446002000104.
48. P. Gong and P. Howarth, "An assessment of some factors influencing multispectral land-cover classification," *Photogrammm Eng. Rem. Sens.* **56**(5), 597–603 (1990).
49. R. G. Congalton and K. Green, "Assessing the accuracy of remotely sensed data: principle and practices," pp. 105–119, Taylor and Francis Groups, CRC Press, Boca Raton, FL (2008).
50. D. P. Rao et al., "IRS-1 A application for land use/land cover mapping in India," *Curr. Sci.* **61**(3–4), 153–161 (1991).
51. J. Adinarayana and N. R. Krishna, "Integration of multiseasonal remotely-sensed images for improved landuse classification of a hilly watershed using geographical information system," *Int. J. Rem. Sens.* **17**(9), 1679–1688 (1996), http://dx.doi.org/10.1080/01431169608948731.
52. Y. Richard and I. Poccard, "A statistical study of NDVI sensitivity to seasonal and inter-annual rainfall variations in Southern Africa," *Int. J. Rem. Sens.* **19**(15), 2907–2920 (1998), http://dx.doi.org/10.1080/014311698214343.
53. S. Rahman, H. Rahman, and M. Keramat, "Study on the seasonal changes of land cover and their impact on surface albedo in the northwestern part of Bangladesh using remote sensing," *Int. J. Rem. Sens.* **28**(5), 1001–1022 (2007), http://dx.doi.org/10.1080/01431160600810880.
54. A. Agresti, *An Introduction to Categorical Data Analysis*, p. 312, Wiley, New York, NY (1996).
55. G. M. Foody, "Remote Sensing of tropical forest environments: towards the monitoring of environmental resources for sustainable development," *Int. J. Rem. Sens.* **24**(20), 4035–4046 (2003), http://dx.doi.org/10.1080/0143116031000103853.
56. P. Sinha, L. Kumar, and N. Reid, "Seasonal variation in land-cover classification accuracy in a diverse region," *Photogramm. Eng. Rem. Sens.* **78**(3), 271–280 (2012).
57. G. Morgan and J. Terrey, *Nature Conservation in Western New South Wale* National Parks Association, Sydney (1992).

Biographies and photographs of the authors are not available.